

Supplementary Information for **Self-Assembled Monolayer Field-Effect Transistors based on Oligo-9,9'-dioctylfluorene Phosphonic Acids**

Bastian Gothe,^a Tjaard de Roo,^b Johannes Will,^c Tobias Unruh^c, Stefan Mecking,^b and Marcus Halik^a

a) Organic Materials & Devices, Institute of Polymer Materials, Department of Materials Science, University Erlangen-Nürnberg, Martensstrasse 7, 91058 Erlangen, Germany

b) Chair of Chemical Materials Science, Department of Chemistry, University of Konstanz, D-78457 Konstanz, Germany

c) Crystallography and Structural Physics, Friedrich-Alexander-Universität Erlangen-Nürnberg, Staudtstrasse 3, 91058 Erlangen, Germany

Experimental Methods

Oligofluorene-phosphonic acid was synthesized according to literature with a final polydispersity index of 1.2.¹ The substance was stored in the dark and handled under ambient conditions. Furthermore, n-octadecylphosphonic acid (C₁₈-PA, purchased from *PCI synthesis*) and 12-Mercaptododecylphosphonic acid (HS-C₁₂-PA purchased from *SiKÉMIA*) were employed.

Devices were built from silicon wafers with 100 nm thermally grown oxide. Gate electrodes were structured with photolithography and wet-etching of 30 nm thick thermally evaporated aluminum. An aluminum oxide layer was formed on top via oxygen-plasma treatment for 5 minutes at 0.2 mbar (Diener Electronic Pico plasma oven, 200W, 40 kHz). This forms an oxide layer² of circa 4 nm which is topped by another deposition of 10 nm aluminum oxide via an atomic layer deposition process (TMA precursor, remote O₂/Ar plasma at 25°C for 30 cycles, Beneq TFS 200) to lower surface roughness. The substrates are activated with a second oxygen plasma treatment and then immersed in a HS-C₁₂-PA solution (0.2 mM in 2-propanol for 24 hours) during which the self-assembled monolayers form. The samples are thoroughly rinsed afterwards with 2-propanol, blown dry with nitrogen and put on a hotplate (60°C) for one minute to remove residual solvent. Source and drain electrodes were patterned from a 30 nm layer of thermally evaporated gold in a photolithographic process and a lift-off step in acetone. For the side-contact layout transistors, the HS-C₁₂-PA SAM is removed from the channel area with the same oxygen plasma treatment as described above. The substrates are then immersed in OF-PA solutions (0.025mM in toluene, 1 hour) and afterwards treated as above, with the exception of an additional ultrasonic treatment (10 seconds) in toluene to remove residual unbound substance.

For structural investigations, silicon wafers were covered with 10 nm aluminum oxide via atomic layer deposition only (parameters as mentioned before). The SAM deposition was carried out

analogous to the earlier described deposition process. This standard procedure has been reported by many groups in the field.²⁻⁶

Characterization

Fluorescence microscopy was done on an *Olympus BX51* microscope with a *X-Cite-120-Q* UV-light source with filters limiting excitation to 330-385 nm and emission to 420 nm and higher.

Contact angles were determined via the Laplace-Young equation for at least ten drops of 2 μl water on a *dataphysics OCA 30* instrument.

Electrical characterization of transistor devices was done with an *Agilent B1500A* parameter analyzer under ambient conditions directly after preparation. For mobility calculations, the capacity was measured to 0.65 $\mu\text{F}/\text{cm}^2$. The saturation mobilities were determined in the saturation regime using the equation:

$$\mu_{sat} = \left(\frac{2L}{WC} \right) \cdot \left(\frac{\partial \sqrt{I_D}}{\partial V_G} \right)^2$$

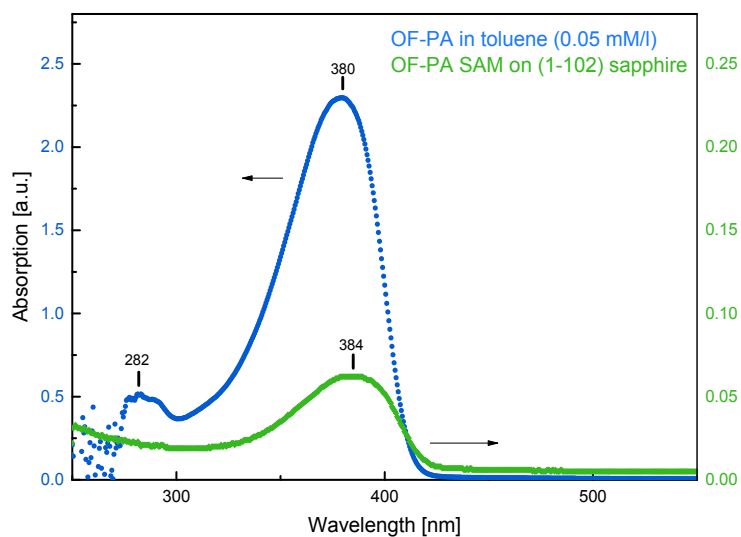
Specular X-ray reflectivity is a surface sensitive and well-established technique^{7,8}, which gives access to the surface normal electron density profile $\rho_e(z)$ of thin films and self-assembled monolayers (SAMs).^{9,10} Here, XRR measurements were performed using a 9 kW Rigaku Smartlab diffractometer with a rotating Cu tube, a Johannsson monochromator and a Goebel mirror. The resulting beam exhibits a characteristic wavelength of 1.54 \AA , a beam height of 0.1 mm and an angular resolution of 0.015°.

The data is analyzed within two approaches. In a first approach, the resulting XRR curves were divided by the intrinsic reflectivity of the substrate, which is called Fresnel reflectivity R_F :⁸

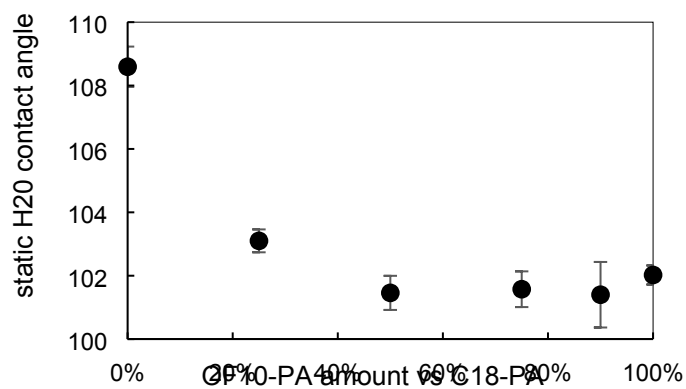
$$R_F(q_z) = \left| \frac{q_z - \sqrt{q_z^2 - q_c^2}}{q_z + \sqrt{q_z^2 - q_c^2}} \right|^2$$

where q_z and q_c are the momentum and the critical momentum transfer vectors normal to the surface and are given by the incidence angle α_z and the critical angle of total reflection α_c via

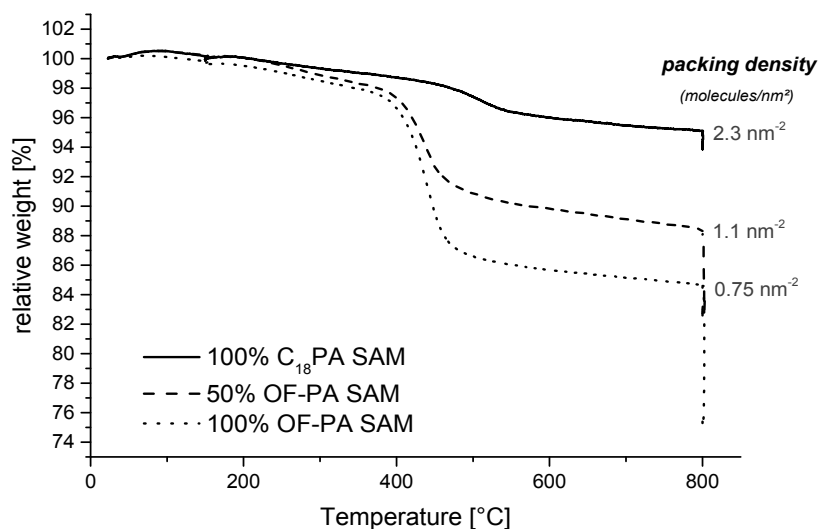
$q_{z/c} = \frac{4\pi}{\lambda} \sin(\alpha_{z/c})$, respectively. Afterwards the 1D Patterson function is calculated from the Fourier transform of the thus Fresnel-normalized reflectivity similar to.¹¹ The resulting Patterson function gives insight into the characteristic length scales present in the investigated sample. In a second approach the XRR data was analysed within the Parratt-formalism¹² utilizing GenX¹³ with a logarithmic figure of merit. The number of introduced slabs was motivated from the 1D Patterson analysis and was successful applied for the better-defined specimens 0% OF-PA, 25% OF-PA and 100% OF-PA.



SI 1 UV-Vis absorption spectra of OF-PA in solution (blue) and surface-bound on sapphire (green). A double-side polished (1-102) sapphire substrate was functionalized with OF10-PA according to the described standard SAM assembly process.



SI 2 Static water contact angles of mixed SAMs assembled on ALD grown AlO_x. Contact angles were determined via the Laplace-Young equation for at least ten drops of 2 μ l water on a *dataphysics OCA 30* instrument.

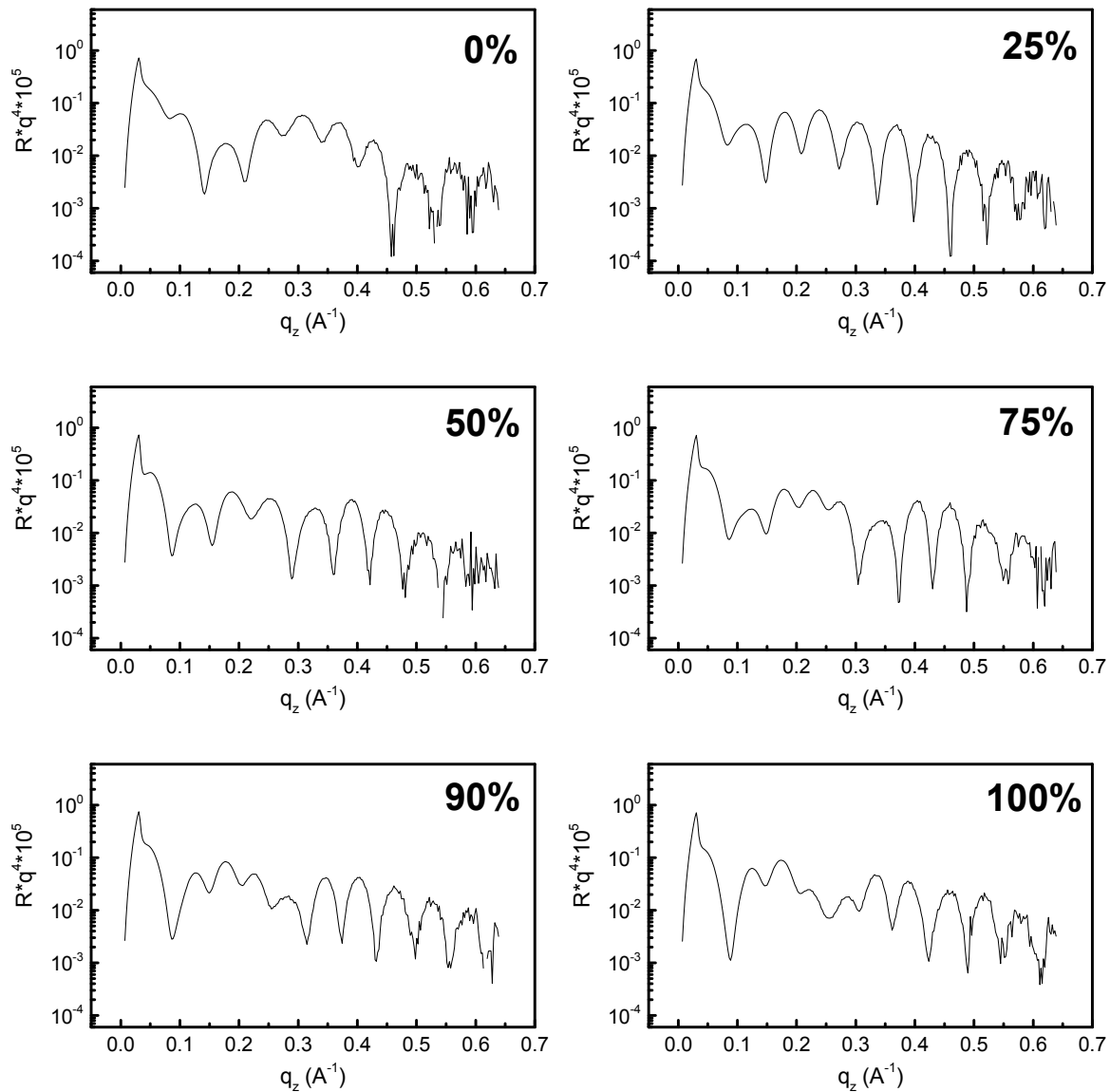


SI 3 Thermogravimetric analysis of OF-PA, C₁₈-PA and mixed SAM bound on 50 nm Al₂O₃ nanoparticles respectively.

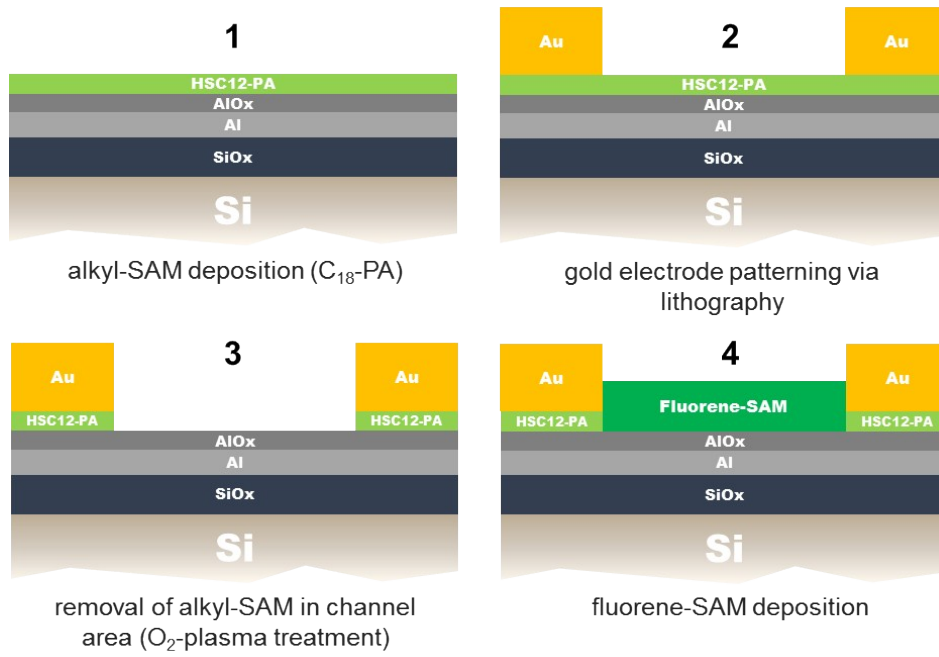
Given grafting densities were determined on the basis of mass loss per specific surface area according to previously reported procedures.¹⁴ Assuming square packing, the 0.75 molecules/nm² determined for 100% OF-PA correspond to an intermolecular distance of 11.5 Å and consequently an electron density of 0.42 e⁻/Å³. The electron density that results from the XRR fits of 100% OF-PA (0.45 e⁻/Å³) is in good agreement with that value.

SI 4 Best fit parameter values defining the electron density profile of OF10-PA.

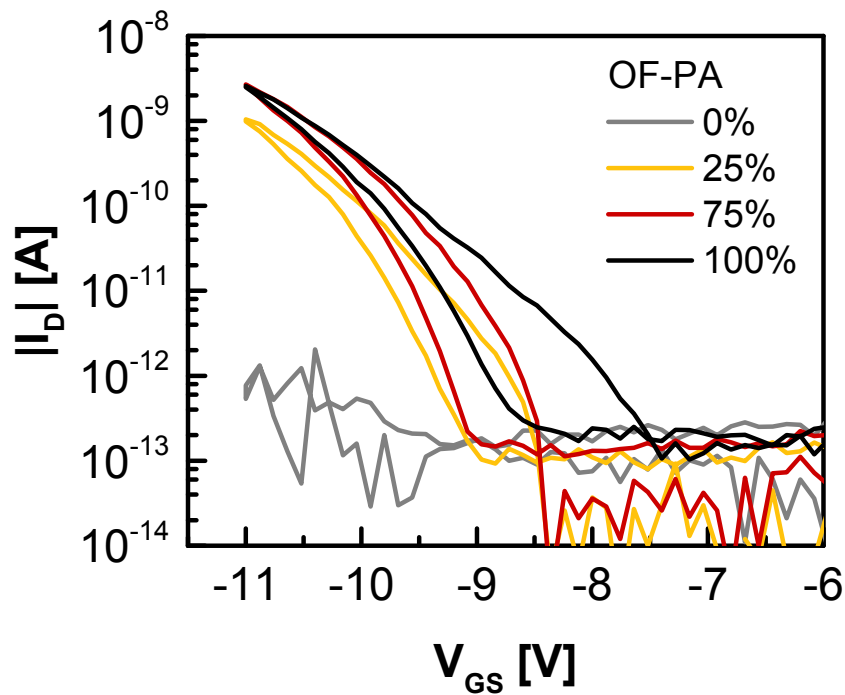
<i>Layer</i>	<i>Unit</i>	<i>0% OF-PA</i> <i>100% C18-PA</i>	<i>25% OF-PA</i> <i>75% C18-PA</i>	<i>100% OF-PA</i> <i>0% C18-PA</i>
SAM2	σ [Å]		5	4.6
	ρ [e ⁻ /Å ³]		0.16	0.45
	d [Å]		10.5	10.8
SAM1	σ [Å]	3.3	4.1	7.8
	ρ [e ⁻ /Å ³]	0.32	0.27	0.18
	d [Å]	19.3	19	11.4
Anchor	σ [Å]	3.2	2.4	2.3
	ρ [e ⁻ /Å ³]	0.94	0.66	0.34
	d [Å]	4	4.4	13.7
AlOx	σ [Å]	3.8	2.3	2.84
	ρ [e ⁻ /Å ³]	0.81	0.81	0.81
	d [Å]	90.8	92.6	90.7
Interface	σ [Å]	4.5	4.8	5.1
	ρ [e ⁻ /Å ³]	0.6	0.51	0.52
	d [Å]	6.7	6.4	6.1
Si	σ [Å]	1.5	1.5	1.5
	ρ [e ⁻ /Å ³]	0.71	0.71	0.71
	d [Å]	∞	∞	∞



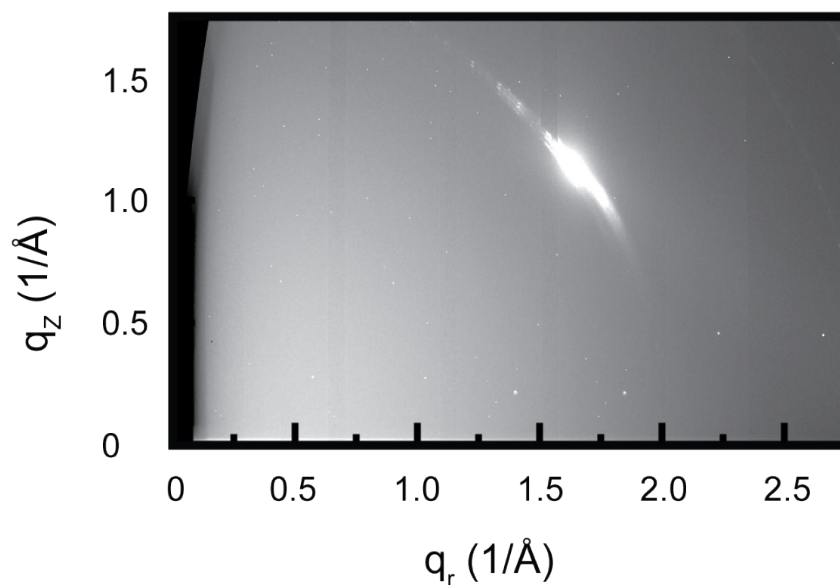
SI 5 X-Ray Reflectivity curves of all mixed SAMs with a ratio of OF-PA versus C₁₈-PA from 0% to 100%. Reflection intensities are normalized for clarity.



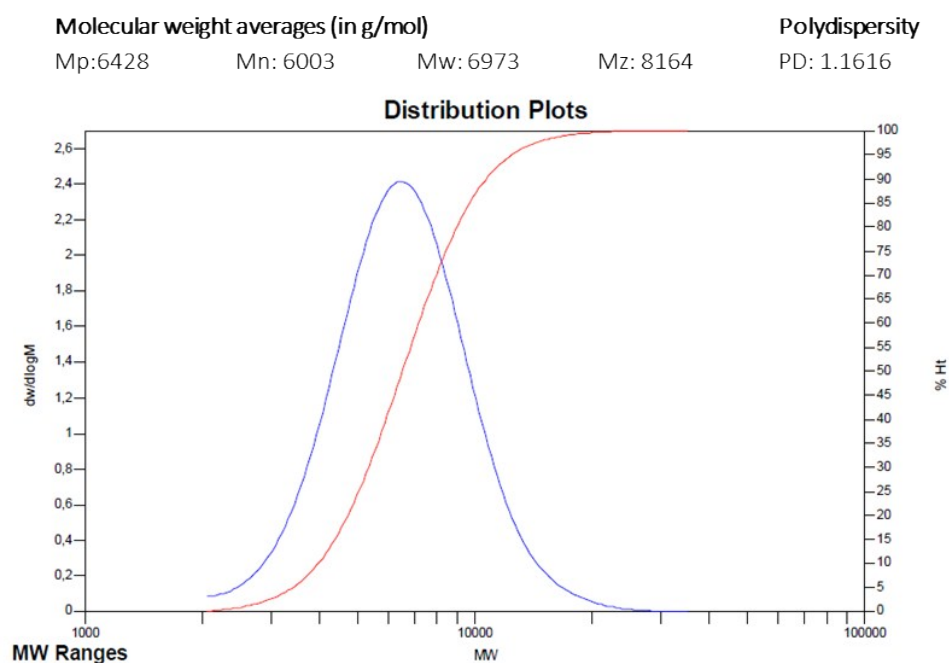
SI 6 Processing steps of the fabrication of the bottom-gate coplanar transistor layout with a thiol-terminated dielectric SAM (HS- C_{12} -PA) and Oligofluorene-PA SAM as the active layer.



SI 7 Transfer curves (saturation regime) of SAMFETs with mixtures of OF-PA with C_{18} -PA at different ratios. Drain voltage I_D was -5 V in all cases. Channels are 100 μm in width and 2 μm in length. The maximum hysteresis is reduced by the addition of an alkyl SAM.



SI 8 Grazing Incidence X-ray Diffraction (GIXD) measurement on OF-PA SAM on 10 nm ALD-grown AlO_x on Si. No Bragg peaks were detected in the diffraction map in (q_r, q_z)-space. Experiments were carried out at beamline ID10 at the European Synchrotron Radiation Facility (ESRF) in Grenoble using 22 keV X-rays. The data was collected with a Pilatus 300 K area detector with an illumination time of 10 s. The incident angle α was set just below the critical angle of silicon. Thus, the X-rays are totally externally reflected, and only the evanescent wave interacts with the sample. In this setup, the scattered intensity from the surface is maximized, whereas the bulk scattering is reduced to a minimum. Some faint vertical bars occur in the diffraction map because the map was created from multiple detector panels.



SI 9 Gel permeation chromatography (GPC) data on the molecular weight distribution of the OF-PA used. The respective polydispersity index (M_w/M_n) amounts to $M_w/M_n < 1.2$. Since molecular weight values from GPC vary with the quality of calibration, Nuclear Magnetic Resonance (NMR) was used for the molecular weight determination which resulted in a number-average M_n of circa 4100 g/mol (10-mer). The measurements were carried out prior to deprotection of the phosphonic acid group. Details on the synthesis and analysis by de Roo et.al can be found in literature.¹

Reference

- 1 T. de Roo, J. Haase, J. Keller, C. Hinz, M. Schmid, D. V. Seletskiy, H. Cölfen, A. Leitenstorfer and S. Mecking, *Adv. Funct. Mater.*, 2014, **24**, 2714–2719.
- 2 A. Jedaa, M. Burkhardt, U. Zschieschang, H. Klauk, D. Habich, G. Schmid and M. Halik, *Org. Electron.*, 2009, **10**, 1442–1447.
- 3 H. Klauk, U. Zschieschang, J. Pflaum and M. Halik, *Nature*, 2007, **445**, 745–8.
- 4 H. Ma, O. Acton, G. Ting, J. W. Ka, H.-L. Yip, N. Tucker, R. Schofield and A. K.-Y. Jen, *Appl. Phys. Lett.*, 2008, **92**, 113303.
- 5 P. H. Wöbkenberg, J. Ball, F. B. Kooistra, J. C. Hummelen, D. M. de Leeuw, D. D. C. Bradley and T. D. Anthopoulos, *Appl. Phys. Lett.*, 2008, **93**, 13303.
- 6 T. Sekitani, T. Yokota, U. Zschieschang, H. Klauk, S. Bauer, K. Takeuchi, M. Takamiya, T. Sakurai and T. Someya, *Science*, 2009, **326**, 1516–9.
- 7 J. (Jean) Daillant and A. Gibaud, *X-ray and Neutron Reflectivity*, Springer Berlin Heidelberg, Berlin, Heidelberg, 2009, vol. 770.
- 8 P. S. Pershan and M. Schlossman, *Liquid Surfaces and Interfaces*, Cambridge University Press, Cambridge, 2012.
- 9 S. R. Wasserman, G. M. Whitesides, I. M. Tidswell, B. M. Ocko, P. S. Pershan and J. D. Axe, *J. Am. Chem. Soc.*, 1989, **111**, 5852–5861.
- 10 A. Khassanov, H.-G. Steinrück, T. Schmaltz, A. Magerl and M. Halik, *Acc. Chem. Res.*, 2015, **48**, 1901–1908.
- 11 X. Chen, T. T. Fister, J. Esbenshade, B. Shi, X. Hu, J. Wu, A. A. Gewirth, M. J. Bedzyk and P. Fenter, *ACS Appl. Mater. Interfaces*, 2017, **9**, 8169–8176.
- 12 L. G. Parratt, *Phys. Rev.*, 1954, **95**, 359–369.
- 13 M. Björck and G. Andersson, *J. Appl. Crystallogr.*, 2007, **40**, 1174–1178.
- 14 L. Zeininger, L. Portilla, M. Halik and A. Hirsch, *Chem. - A Eur. J.*, 2016, **22**, 13506–13512.